Chemistry and Materials

The Center for Science Innovation

Research Article

Chem. Mater. 3 (3) 2024, 90-97

Additive-free Electrodeposition of SnCoNi Trimetallic Catalysts for Ethanol Electrooxidation

Qori'atun Ni'mah Salsabila[1,*], Fabian Glorious Kenaya[1], Muhammad Fathar Aulia[2], Muhammad Athariq[2]

[1]Department of Chemistry, Faculty of Mathematics and Natural Science, Universitas Negeri Jakarta, Jalan Rawamangun Muka, Jakarta 13220, Indonesia

[2]The Center for Science Innovation, East of Jakarta 13120, Indonesia

*Corresponding author: qoriatunnimah@gmail.com

Received
9 September 2024

Received in revised form
10 October 2024

Accepted
13 October 2024

Published online
31 October 2024

DOI
https://doi.org/10.56425/cma.v3i3.84

Abstract

SnCoNi catalysts were synthesized via electrodeposition, with and without citric acid, to assess their ethanol electrooxidation performance. The additive-free catalyst exhibited superior properties, including lower charge transfer resistance and a smaller Tafel slope compared to the citric acid-modified catalyst. Chronoamperometry testing further revealed better electrochemical stability for the additive-free catalyst, with less current loss over time. Cyclic voltammetry confirmed the enhanced ethanol oxidation activity with a relatively high current density. The improved performance is attributed to better mass transport, active site exposure, and the synergistic effects of Sn, Co, and Ni in the additive-free catalyst, making it more efficient for ethanol electrooxidation. These findings suggest that the additive-free catalyst exhibits more favorable properties for ethanol electrooxidation compared to its citric acid-modified counterpart.

Keywords: electrodeposition, ethanol electrooxidation, electrocatalyst

1. Introduction

Alcohol fuel cells are a promising, clean, and powerful alternative to fossil fuels [1]. As a direct fuel for fuel cells, ethanol has a higher theoretical mass-energy density than methanol (8.0 vs. 6.1 kWh/kg) [2], offering better storage security and lower production and handling costs. Additionally, ethanol is more economical than methanol because it can be produced on a large scale from the agricultural sector and has lower toxicity [2–3].

In a direct ethanol fuel cell (DEFC), the anode reaction is the ethanol oxidation reaction (EOR), which involves the transfer of 12 electrons for the complete oxidization of ethanol into CO_2 [4]. However, its slow kinetics and imperfect oxidations are problematic, thus reducing the current density and inhibiting the application of DEFC. The overall oxidation of ethanol is given below [5].

$$C_2H_5O + 3H_2O \longrightarrow CO_2 + 6H^+ + 6e^- \quad (1)$$

$$3O_2 + 12H^+ + 12e^- \longrightarrow 6H_2O \quad (2)$$

Electrocatalysts that are known to have good efficiency for EOR are noble metal-based materials such as Pt, Pd, and Au, which exhibit exceptional catalytic activity [6]. However, some disadvantages of these metals for DEFC applications are their relatively high prices. Additionally, they are susceptible to poisoning from intermediate species generated during the reaction. Consequently, it is essential to develop strategies to mitigate these issues [7].

Electrocatalysts based on transition metal materials have been extensively developed. Ni is a highly proposed transitional metal because of its advantages as an electrocatalyst, including good electrocatalyst activity and stability, as well as its high degree of alloying with other metals [8]. A previous study has demonstrated that CoNi alloys exhibit superior catalytic efficiency for alcohol electrooxidation compared to pure nickel [9]. In another study, the modification of Pt with Sn and SnNi improved ethanol and carbon monoxide electro-oxidation [10]. The incorporation of Co and Sn into the Ni grid can improve the stability of the element [11]. This approach leverages the synergistic effects among nickel, cobalt, and tin, as well as the trimetallic properties of SnCoNi, to produce electrocatalysts with enhanced activity and efficiency.

In ethanol electrooxidation, the catalyst additives are widely used to enhance catalytic activity and stability and modify the particle structure as desired [12]. Common

catalyst additives for support materials like carbon-based materials, metal oxides, hydroxides, carbides, and sulfides. Consider research found the addition of metal oxides, like TiO_2, in a catalyst can improve stability during EOR [13]. Citric acid is one of the additives used to protect substrates from corrosion by creating a protective layer that can reduce the corrosion rate of electrodes and substrates [14]. However, the formation of unwanted by-products, the risk of environmental hazards, and increased production costs hinder its use for large-scale production [15].

The electrodeposition method is considered one of the most suitable methods for preparing metal and alloy catalysts. This is because the electrocatalyst obtained through electrodeposition has good electrical conductivity and cost-effectiveness, and the catalyst morphology can be adjusted effectively to obtain an electrode structure with the desired active site exposure [16–17].

In this study, SnCoNi catalysts were prepared using electrodeposition methods, both with and without the addition of citric acid. The purpose of this research is to develop an additive-free SnCoNi catalyst with high catalytic activity for the electrooxidation of ethanol by comparing its performance to that of a citric acid-modified counterpart.

2. Materials and Method

2.1 Synthesis of SnCoNi electrocatalyst

SnCoNi electrocatalyst was prepared using $NiSO_4.6H_2O$, $CoSO_4.7H_2O$, and $SnCl_2$ by the electrodeposition method of the potentiostat technique in a three-electrode system. SnCoNi was made with the addition of citric acid compared to SnCoNi without citric acid and tested to see its effect on the properties and characteristics of the resulting catalyst. The copper wire substrate was prepared before being washed using technical ethanol and distilled water.

The process of preparing a SnCoNi catalyst by electrodeposition on a copper wire substrate is as follows: the electrodeposition process is carried out in a three-electrode system with copper wire as the working electrode, Pt as the counter electrode, and Ag/AgCl as the reference electrode inserted into the electrodeposition cell. The electrolytes were made as much as 25 mL consisting of 0.07 M $NiSO_4 \cdot 6H_2O$, 0.02 M $CoSO_4 \cdot 7H_2O$, 0.01 M $SnCl_2$, 0.04 M, H_3BO_3, and 0.1 M H_2SO_4. Electrodeposition was performed at room temperature at a potential of -1.4 V vs. Ag/AgCl for 600 s. Under the same conditions, prepared citric acid was added to the electrolyte for comparison.

2.2 Characterization

The crystallographic structure of samples was investigated by X-ray diffraction (XRD), scanning electron microscopy (SEM), and energy dispersive X-ray (EDX) was performed to analyze the morphological characteristics and microstructure of catalysts. The particle size distributions were determined by measuring the particle using image tool software.

2.3 Electrochemical test

Electrochemical measurements were performed in a standard three-electrode electrochemical cell using an electrochemical workstation, with Pt and Ag/AgCl used as the counter electrode and reference electrode, respectively. The copper wire substrate covered with the electrodeposited film served as the working electrode.

Electrochemical impedance spectroscopy (EIS) analysis was used to determine the electron transfer resistance (R_{ct}) of samples. EIS analysis was measured at a frequency of 100 kHz-0.1 Hz in a 0.5 M KCl solution. Cyclic voltammetry (CV) and chronoamperometry measurements were performed to investigate the activity and stability of samples for EOR. CV analysis was conducted in a 0.5 M NaOH and 1 M ethanol solution. The potential used is between -750 mV and 750 mV at a scan rate of 100 mV/s. Linear sweep voltammetry (LSV) curves were measured at a scan rate of 100 mV/s. The stability tests of samples were performed for EOR with a constant voltage of 0.3 V vs. Ag/AgCl for 3,600 s.

3. Results and Discussion

3.1 Characterization

The XRD patterns of SnCoNi samples synthesized with citric acid (CA) and without citric acid (WCA) are presented in Fig. 1. The sample prepared in the presence of citric acid sample (black line) exhibits sharper and more intense peaks compared to the without citric acid sample (red line), indicating a higher degree of crystallinity [18]. The addition of citric acid appears to facilitate improved crystallization. By comparing the diffraction peaks with standard reference patterns for SnCoNi (COD-152-4151), Tin (COD-900-8571), Cobalt (COD-901-1625), and Nickel (COD-901-3034), the phases present in each sample can be identified.

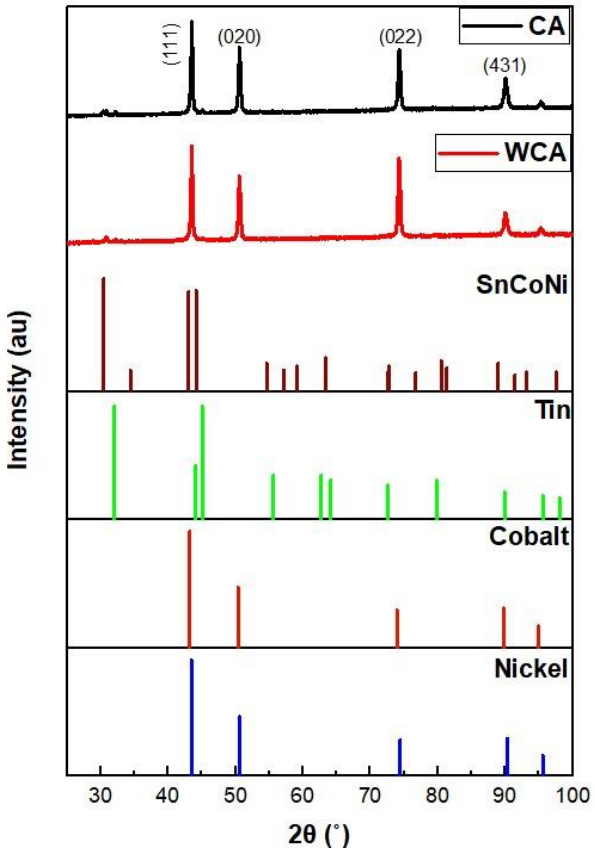

Figure 1. XRD patterns of SnCoNi and the Crystal Open Database patterns for Ni, Co, Sn and SnCoNi alloy.

The citric acid sample aligns predominantly with the SnCoNi standard, suggesting the formation of a well-defined SnCoNi phase. In contrast, the sample synthesized without citric acid exhibits additional or shifted peaks, suggesting the presence of new crystalline phases or impurities due to the absence of citric acid during synthesis [19].

Figure 2 illustrates the distinct morphologies of SnCoNi catalysts synthesized with and without citric acid. The SEM image of the catalyst prepared with citric acid shows a well-organized, fishbone-like structure, characterized by a central spine with regularly spaced branches. This morphology results from citric acid acting as a complexing agent, controlling metal ion deposition and promoting anisotropic growth that leads to a more defined structure. In contrast, the catalyst synthesized without citric acid exhibits a more compact, cauliflower-like morphology. The absence of citric acid leads to a less controlled deposition process, resulting in aggregated and irregular structures with a rougher surface [20].

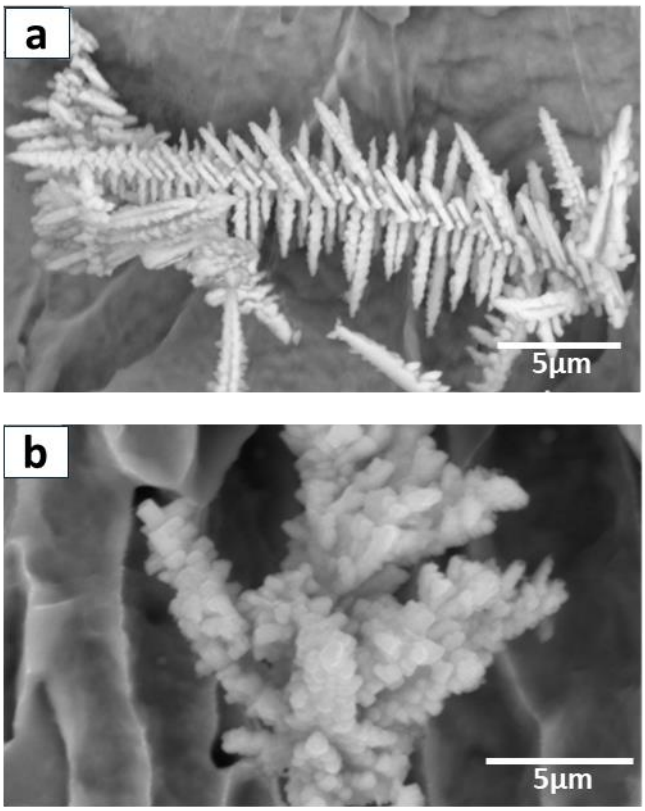

Figure 2. SEM and size distribution of (a) SnCoNi with citric acid, (b) SnCoNi without citric acid.

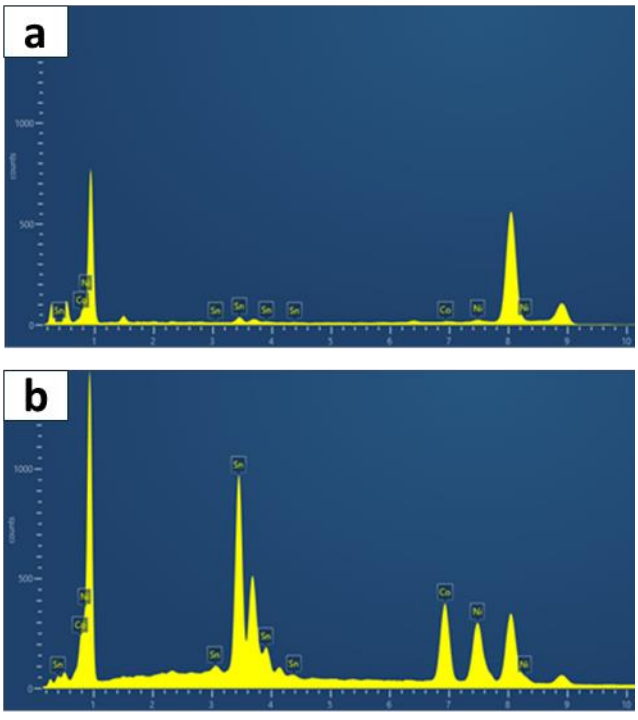

Figure 3. EDX spectrum of SnCoNi (a) with citric acid and (b) without citric acid.

These morphological differences are likely to influence the catalytic performance in ethanol electrooxidation. The fishbone-like structure, with its regular and elongated features, might offer fewer active sites but could facilitate efficient electron transfer along the well-defined pathways [21]. On the other hand, the cauliflower-like morphology, with its rough and irregular surface, might provide a higher density of exposed active sites and potentially more surface defects, which could enhance catalytic activity.

The EDX spectrum in Fig. 3 confirmed the presence of elements Sn, Co, and Ni. The elemental ratio of SnCoNi samples is presented in Table 1.

Table 1. Ratio wt% of SnCoNi samples.

Sample	wt%		
	Sn	Co	Ni
SnCoNi with citric acid	79.20%	10.50%	16.60%
SnCoNi without citric acid	51.46%	27.42%	21.12%

3.2 Electrochemical performance of electrocatalyst towards EOR

The electrocatalyst in the DEFC system provides a surface on which the electrooxidation of ethanol occurs at lower activation energy and a higher rate. Lower activation energy significantly reduces the energy consumed during the breaking and formation of reactant and product bonds, and a higher reaction rate minimizes the time required for the reaction to occur [22]. In the DEFC system, CO_2 is the expected product. The CO_2 released during the production and oxidation process of ethanol can be utilized by biomass-producing plants, thus completing CO_2 production and making DEFC harmless to the environment [1].

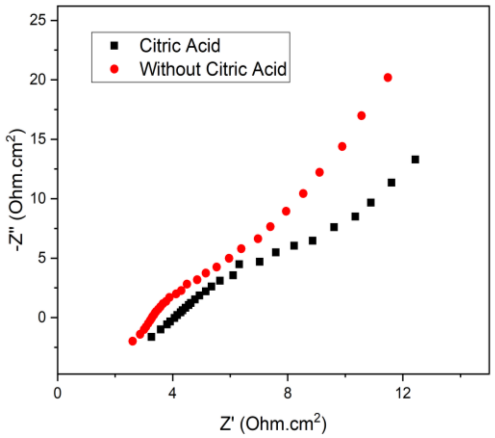

Figure 4. Nyquist plot of SnCoNi with citric acid and without citric acid.

To properly investigate the electrocatalytic activity of SnCoNi for EOR, it was evaluated with EIS. EIS analysis is used to determine charge resistance transfer R_{ct} [23]. R_{ct} is the resistance to the transfer of ions from a solvated ionic state in the electrolyte across the electrode interface into the electrode, which causes the activation polarization [24]. The value of R_{ct} is represented by a semicircle-shaped Nyquist plot [25]. Figure 5 shows the Nyquist plot of the SnCoNi samples.

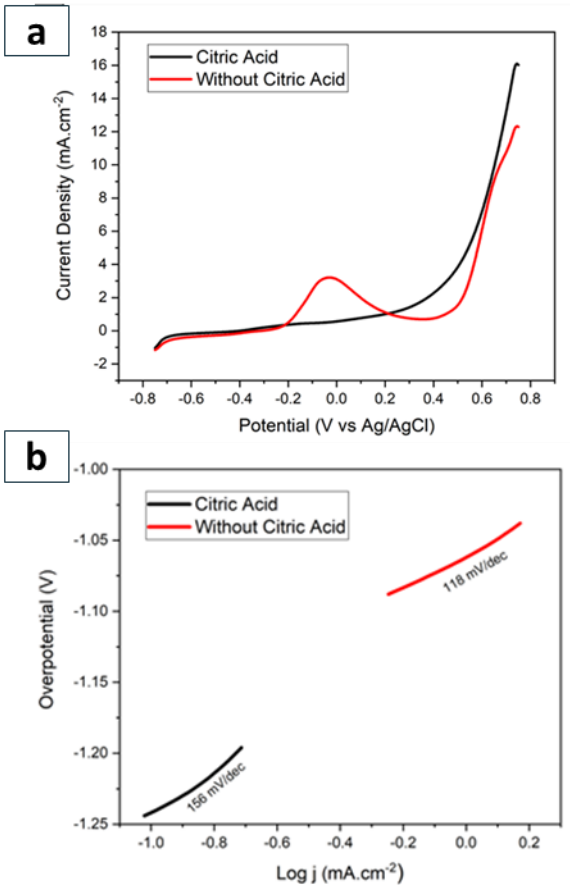

Figure 5. (a) LSV curves of SnCoNi samples (b) corresponding Tafel plots.

Figure 4 shows the Nyquist plot of the SnCoNi samples. SnCoNi without citric acid has an R_{ct} of 11.85 Ω which is smaller than SnCoNi with citric acid which has an R_{ct} value of 19.12 Ω shown in Table 2. The smaller R_{ct} value indicates the best electron transfer capability at the interface between the electrode and the electrolyte [4]. This is because SnCoNi without adding citric acid are more tightly distributed. In contrast, SnCoNi with added citric acid exhibits a much higher R_{ct} due to its low activity. The larger semicircle diameter in the higher frequency region corresponds to R_{ct} of SnCoNi without citric acid confirming better interfacial charge transfer ability [26].

Table 2. Solution resistance (R_s) and charge transfer resistance (R_{ct}) from Nyquist plot.

Sample	R_s	R_{ct}
SnCoNi With Citric Acid	4.19 Ω	19.12 Ω
SnCoNi Without Citric Acid	3.32 Ω	11.85 Ω

The LSV curves in Fig. 5a show the onset potential of EOR on the prepared catalyst. The LSV curve shows that SnCoNi without citric acid shows a lower onset potential compared to SnCoNi with citric acid. The lower onset potential indicates a significant enhancement in EOR [27]. In Fig. 5b, the Tafel slopes for SnCoNi with and without citric acid are 158 mV/dec and 118 mV/dec, respectively. The SnCoNi without citric acid exhibits the smallest Tafel slope, indicating that it is a more active catalyst, as a smaller overpotential is required to achieve a higher current density [28].

Table 3. Comparison of current densities on metal-based catalysts.

Catalyst	Electrolyte	j (mA.cm^{-2})	Ref
Pt-NiO/C	1 M KOH + 1 M Ethanol	11.5	[29]
NiPd/Ti	1 M KOH + 1 M Ethanol	2.5	[30]
Pd/SnO_2-TiO_2/CNT	0.5 M NaOH + 1 M Ethanol	1.48	[31]
CoNi	0.1 M KOH + 0.1 M Ethanol	3.14	[23]
SnCoNi	0.5 M NaOH + 1 M ethanol	3.11	This study

To further investigate the electrochemical properties of trimetallic SnCoNi, EOR analysis was conducted using chronoamperometry technique. The detailed results, highlighting the catalysts performance and stability over time, are presented in Fig 6.

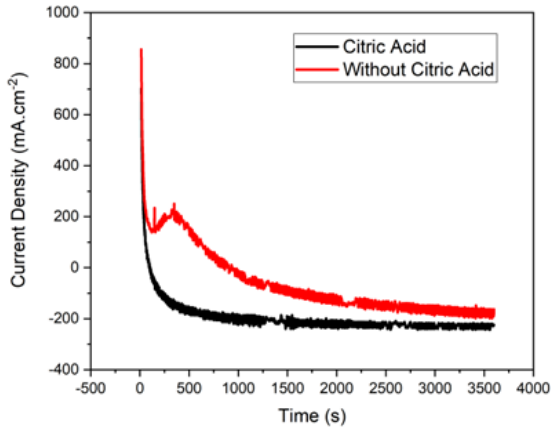

Figure 6. Chronoamperometry curves of SnCoNi electrocatalyst.

The electrochemical stability of the SnCoNi electrocatalyst was evaluated using the chronoamperometry technique by applying a potential of 0.3 V vs. Ag/AgCl for 3,600 s. The SnCoNi with citric acid shows a significant current loss compared to SnCoNi without citric acid, exhibiting much better electrocatalytic stability of the synthesized SnCoNi due to the synergetic effect of Ni, Co, and Sn metals.

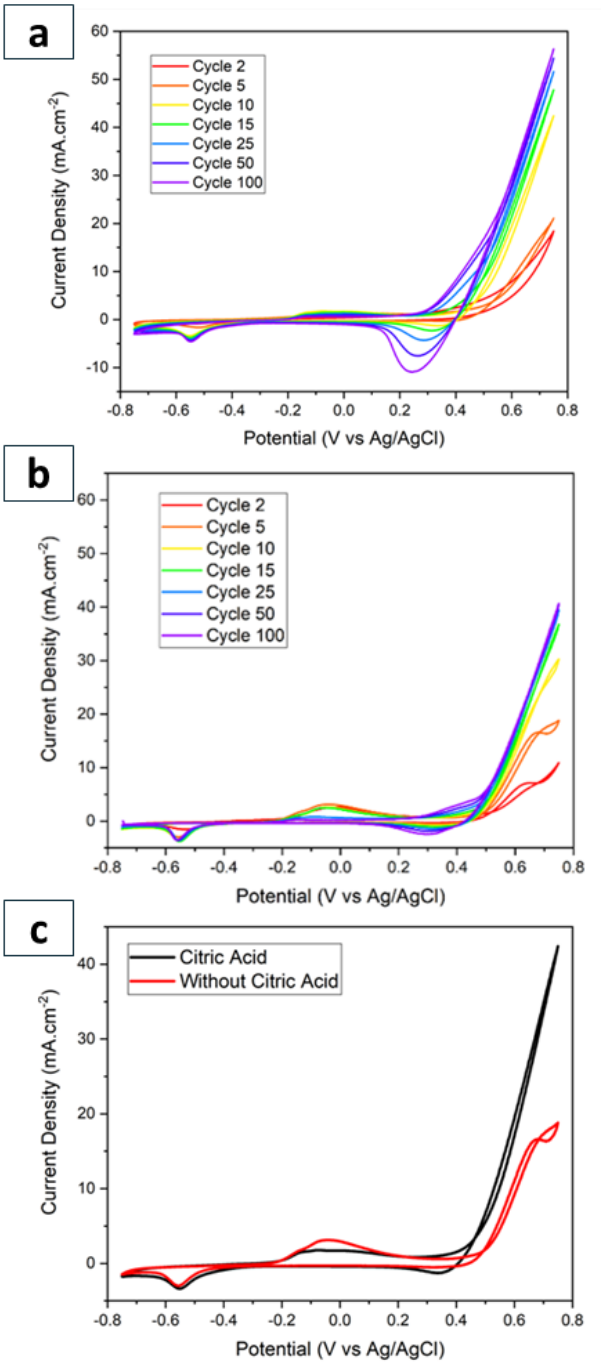

Figure 7. CV curves of SnCoNi (a) with citric acid, (b) without citric acid, and (c) curves with highest peak intensity.

Furthermore, to evaluate the electrochemical performance of the as-synthesized catalysts towards EOR, CV tests were conducted. Figure 7 shows the CV diagrams of the SnCoNi electrocatalyst in 0.5 M NaOH and 1.0 M ethanol solutions. The CV results produce a current density during the forward scan (j_f) of SnCoNi with citric acid and without citric acid, respectively, at 2.09 mA/cm² and 3.11 mA/cm². Comparison of current densities on metal-based catalysts is shown in Table 3.

The CV plot illustrates the relationship between current density and potential, measured against a reference electrode. When ethanol is present in the electrolyte solution, an increase in current density can be observed, which indicates the occurrence of ethanol electrooxidation [32].

CV analysis showed a decrease in current density along with the addition of cycles in both SnCoNi with and without citric acid. The SnCoNi catalyst without citric acid exhibits resistance to EOR ability at 50% of the initial activity, and SnCoNi with citric acid exhibits stability to EOR 30% after 100 cycles, which confirms better stability for the catalyst without the addition of an additive [23]. The observed phenomenon indicates a consistent decline in current over successive CV cycles. This observation implies that carbon monoxide poisoning may be affecting the catalyst surface or that structural damage is occurring due to the aggregation or distortion of the CoNi catalyst [33].

SnCoNi without citric acid presents defined oxidation peaks with greater current density. Both citric acid and low pH conditions can contribute to catalyst poisoning [34]. Intermediates formed during ethanol oxidation may adsorb strongly onto the catalyst surface, blocking active sites and reducing overall activity. This phenomenon can be exacerbated in environments with high acidity or improper catalyst formulations involving citric acid [35].

Table 4. The ratio of j_b/j_f SnCoNi electrocatalysts.

SnCoNi	j (mA.cm^{-2})		
	j_f	j_b	j_b/j_f
With Citric Acid	2.09	3.85	1.84
Without Citric Acid	3.11	2.81	0.90

The ratio between the current density of backward and forward scans (j_b/j_f) can indicate the performance of the electrocatalyst. The smaller ratio of j_b/j_f exhibited better performance of the electrocatalyst in facilitating the ethanol electrooxidation process [36]. Based on Table 4, SnCoNi without citric acid has the lowest j_b/j_f value, which indicates the potential for CO_{ads} poisoning tolerance compared to SnCoNi with citric acid.

4. Conclusion

The study demonstrates that the additive-free SnCoNi catalyst exhibits superior properties in electrochemical tests. Without citric acid, SnCoNi shows greater current density and stability in ethanol oxidation, as indicated by CV results. The absence of a catalyst additive likely enhances CV activity. In LSV tests, SnCoNi without citric acid has a lower onset potential and a smaller Tafel slope (118 mV/dec) compared to the citric acid-modified catalyst (158 mV/dec), indicating higher activity due to lower overpotential. Nyquist plots reveal that SnCoNi without citric acid has the smallest charge transfer resistance, reflecting superior electron transfer at the electrode-electrolyte interface. Chronoamperometric tests confirm that it maintains better electrocatalytic stability over 3,600 seconds, attributed to the synergistic effects of Ni, Co, and Sn. Overall, EIS, LSV, CV, and chronoamperometry results consistently indicate that SnCoNi without citric acid outperforms its citric acid-containing counterpart. Scanning electron microscopy (SEM) imaging further reveals morphological differences likely linked to this improved electrochemical performance.

Acknowledgement

The authors thank DRTPM Kemendikbudristek for supporting this work under Penelitian Terapan Kompetitif Nasional research scheme 2023.

References

[1] A.N. Vyas, G.D. Saratale, S.D. Saratale, Recent developments in nickel-based electrocatalysts for ethanol electrooxidation, *International Journal of Hydrogen Energy.* **45** (2020) 5928–5947. https://doi.org/10.1016/j.ijhydene.2019.08.218

[2] L. Yaqoob, T. Noor, N. Iqbal, A comprehensive and critical review of the recent progress in electrocatalysts for the ethanol oxidation reaction, *RSC Advances.* **11** (2021) 16768–16804. https://doi.org/10.1039/D1RA01841H

[3] J. Tayal, B. Rawat, S. Basu, Bi-metallic and tri-metallic Pt–Sn/C, Pt–Ir/C, Pt–Ir–Sn/C catalysts for electro-oxidation of ethanol in direct ethanol fuel cell, *International Journal of Hydrogen Energy.* **36** (2011) 14884–14897. https://doi.org/10.1016/j.ijhydene.2011.03.035

[4] H. Syafei, D.I. Syafei, Square-Wave Pulse Deposition of Pt Nanoparticles for Ethanol Electrooxidation, *Chem. Mater*. **3** (2024) 21-26. https://doi.org/10.56425/cma.v3i1.70

[5] G. Yang, Q. Zhang, H. Yu, F. Peng, Platinum-based ternary catalysts for the electrooxidation of ethanol, *Particuology.* **58** (2021) 169–186. https://doi.org/10.1016/j.partic.2021.01.007

[6] S. Wei, F. Xie, M. Gan, L. Ma, T. Wu, Q. Fu, T. Li, Y. Yang, W. Zhan, A highly-efficient and durable Pt-based electrocatalyst decorated by Co2C-Mo2C@CS composite for methanol oxidation reaction, *Synthetic Metals.* **280** (2021) 116878. https://doi.org/10.1016/j.synthmet.2021.116878

[7] K.X. Zhang, Z.P. Liu, Electrochemical hydrogen evolution on Pt-based catalysts from a theoretical perspective, *The Journal of Chemical Physics.* **158** (2023). https://doi.org/10.1063/5.0142540

[8] K. Rahmani, B. Habibi, Excellent electro-oxidation of methanol and ethanol in alkaline media: Electrodeposition of the NiMoP metallic nanoparticles on/in the ERGO layers/CE, *International Journal of Hydrogen Energy.* **45** (2020) 27263–27278. https://doi.org/10.1016/j.ijhydene.2020.07.110

[9] X. Tarrús, M. Montiel, E. Vallés, E. Gómez, Electrocatalytic oxidation of methanol on CoNi electrodeposited materials, *International Journal of Hydrogen Energy.* **39** (2014) 6705–6713. https://doi.org/10.1016/j.ijhydene.2014.02.057

[10] N. Hidayati, K. Scott, Electro-oxidation of Ethanol on Carbon Supported PtSn and PtSnNi Catalysts, *Bulletin of Chemical Reaction Engineering & Catalysis*. **11** (2016) 10-20. https://doi.org/10.9767/bcrec.11.1.399.10-20

[11] Y. Liu, H. Lu, X. Kou, Electrodeposited Ni-Co-Sn alloy as a highly efficient electrocatalyst for water splitting, *International Journal of Hydrogen Energy.* **44** (2019) 8099–8108. https://doi.org/10.1016/j.ijhydene.2019.02.078

[12] F. Chen, J. Liang, F. Wang, X. Guo, W. Gao, Y. Kugue, Y. He, G. Yang, P. Reubroycharoen, T. Vitidsant, N. Tsubaki, Improved catalytic activity and stability of Cu/ZnO catalyst by boron oxide modification for low-temperature methanol synthesis, *Chemical Engineering Journal*. **458** (2023) 141401. https://doi.org/10.1016/j.cej.2023.141401

[13] Y. Zheng, X. Wan, X. Cheng, K. Cheng, Z. Dai, Z. Liu, Advanced Catalytic Materials for Ethanol Oxidation in Direct Ethanol Fuel Cells, *Catalysts*. **10** (2020) 166. https://doi.org/10.3390/catal10020166

[14] J. Wysocka, S. Krakowiak, J. Ryl, Evaluation of citric acid corrosion inhibition efficiency and passivation kinetics for aluminium alloys in alkaline media by means of dynamic impedance monitoring, *Electrochimica Acta.* **258** (2017) 1463–1475. https://doi.org/10.1016/j.electacta.2017.12.017

[15] M.A. Basyooni-M Kabatas, A Comprehensive Review on Electrocatalytic Applications of 2D Metallenes, *Nanomaterials*. **13** (2023) 2966. https://doi.org/10.3390/nano13222966

[16] B. Subramanian, K. Govindan, V. Swaminathan, M. Jayachandran, Materials properties of electrodeposited NiFe and NiCoFe coatings, *Transactions of the IMF.* **87** (2009) 325–329. https://doi.org/10.1179/174591909X12554332311546

[17] Y. Qian, M. Hu, L. Li, S. Cao, J. Xu, J. Hong, X. Liu, J. Xu, C. Guo, Dynamically assisted electrodeposition by hydrogen bubbles on carbonized wood: A NiFeCo nanoflower electrocatalyst for efficient hydrogen evolution, *Fuel.* **361** (2024) 130653. https://doi.org/10.1016/j.fuel.2023.130653

[18] Z.Q. Li, C.J. Lu, Z.P. Xia, Y. Zhou, Z. Luo, X-ray diffraction patterns of graphite and turbostratic carbon, *Carbon.* **45** (2007) 1686–1695. https://doi.org/10.1016/j.carbon.2007.03.038

[19] A. Sharma, S. Bhattacharya, S. Das, K. Das, Influence of current density on surface morphology and properties of pulse plated tin films from citrate electrolyte, *Applied Surface Science.* **290** (2014) 373-380. https://doi.org/10.1016/j.apsusc.2013.11.088

[20] G. M. Zarkadas, A. Stergiou, G. Papanastasiou, Influence of citric acid on the silver electrodeposition from aqueous AgNO3 solutions, *Electrochimica Acta.* **50** (2005) 5022–5031. https://doi.org/10.1016/j.electacta.2005.02.081

[21] K. Duangsa, A. Tangtrakarn, C. Mongkolkachit, P. Aungkavattana, K. Moolsarn, The Effect of Tartaric Acid and Citric Acid as a Complexing Agent on Defect Structure and Conductivity of Copper Samarium Co-Doped Ceria Prepared by a Sol-Gel Auto-Combustion Method, *Advances in Materials Science and Engineering.* **44** (2021) 1-23. https://doi.org/10.1155/2021/5592437

[22] M.A.F. Akhairi, S.K. Kamarudin, Catalysts in direct ethanol fuel cell (DEFC): An overview. *International Journal of Hydrogen Energy.* **41** (2016) 4214–4228. https://doi.org/10.1016/j.ijhydene.2015.12.145

[23] A.A. Fazri, A.N. Puspita, S. Ningsih, A. Auliya, Electrodeposition of CoNi Bimetallic Catalyst for Ethanol Electrooxidation Application, *Chem. Mater*. **2** (2023) 56-60. https://doi.org/10.56425/cma.v2i3.63

[24] T.R. Jow, M.B. Marx, J.L. Allen, Distinguishing Li^+ Charge Transfer Kinetics at NCA/Electrolyte and Graphite/Electrolyte Interfaces, and NCA/Electrolyte and LFP/Electrolyte Interfaces in Li-Ion Cells, *Journal of The Electrochemical Society.* **159** (2012) A604–A612. https://doi.org/10.1149/2.079205jes

[25] F. Lou, D. Chen, Aligned carbon nanostructures based 3D electrodes for energy storage, *Journal of Energy Chemistry.* **24** (2015) 559–586. https://doi.org/10.1016/j.jechem.2015.08.013

[26] L. Qin, J. Lian, Q. Jiang, Effect of grain size on corrosion behavior of electrodeposited bulk nanocrystalline Ni, *Transactions of Nonferrous Metals Society of China.* **20** (2010) 82–89. https://doi.org/10.1016/S1003-6326(09)60101-1

[27] Q. Zhang, T. Chen, R. Jiang, F. Jiang, Comparison of electrocatalytic activity of Pt_{1-x} Pd $_x$/C catalysts for ethanol electro-oxidation in acidic and alkaline media. *RSC Adv*. 10 (2020) 10134-10143. https://doi.org/10.1039/d0ra00483a

[28] A. Raveendran, M. Chandran, R, Dhanusuraman, A comprehensive review on the electrochemical parameters and recent material development of electrochemical water splitting electrocatalysts, *RSC Advances.* **13** (2023) 3843–3876.

[29] F. Hu, C. Chen, Z. Wang, G. Wei, P.K. Shen, Mechanistic study of ethanol oxidation on Pd–NiO/C electrocatalyst, Electrochim. Acta. **52** (2006) 1087–1091. https://doi.org/10.1016/j.electacta.2006.07.008

[30] J. Rosario, J. Ocon, H. Jeon, Y. Yi, J. Lee, J. Lee, Enhancing Role of Nickel in the Nickel-Palladium Bilayer for Electrocatalytic Oxidation of Ethanol in Alkaline Media, *J. Phys. Chem. C.* **118** (2014) 22473–22478. https://doi.org/10.1021/jp411601c

[31] C.A. López-Rico, J. Galindo-de-la-Rosa, E. Ortiz-Ortega, L. Álvarez-Contreras, J. Ledesma-García, M. Guerra-Balcázar, L.G. Arriaga, N. Arjona, High performance of ethanol co-laminar flow fuel cells based on acrylic, paper and Pd-NiO as anodic catalyst, *Electrochim. Acta.* **207** (2016) 164–176. https://doi.org/10.1016/j.electacta.2016.05.002

[32] A. Cuña, C. Reyes Plascencia, E.L. da Silva, J. Marcuzzo, S. Khan, N. Tancredi, M.R. Baldan, C. de Fraga Malfatti, Electrochemical and spectroelectrochemical analyses of hydrothermal carbon supported nickel electrocatalyst for ethanol electro-oxidation in alkaline medium, *Applied Catalysis B: Environmental.* **202** (2017) 95– https://doi.org/10.1016/j.apcatb.2016.08.063

[33] D. Chung, H. Kim, Y. Chung, Inhibition of CO poisoning on Pt catalyst coupled with the reduction of toxic hexavalent chromium in a dual-functional fuel cell, *Scientific Reports*. **4** (2014). https://doi:10.1038/srep07450

[34] S. Sun, Z. Jusys, R.J. Behm, Electrooxidation of ethanol on Pt-based and Pd-based catalysts in alkaline electrolyte under fuel cell relevant reaction and transport conditions, *Journal of Power Sources.* **231** (2013) 122–133. https://doi.org/10.1016/j.jpowsour.2012.12.091

[35] W. Chaitree, E.E. Kalu, Z. Liang, Yaw. D. Yeboah, Effects of bath composition and thermal treatment on the performance of Co-Ni-Mo-P electrocatalyst supported on carbon for the electro-oxidation of ethanol, *Journal of Alloys and Compounds.* **860** (2021) 158404. https://doi.org/10.1016/j.jallcom.2020.158404

[36] A. Sabella, R. Syifa, N.A. Dwiyana, The Effect of Deposition Potential on the Electrodeposition of Platinum Nanoparticles for Ethanol Electrooxidation, *Chem. Mater*. **1** (2022) 88-92. https://doi.org/10.56425/cma.v1i3.46